



Plutonium concentrations link soil organic matter decline to wind erosion in ploughed soils of South Africa

Joel Mohren^{1,2*}, Hendrik Wiesel^{3,4}, Wulf Amelung⁵, L. Keith Fifield⁶, Alexandra Sandhage-Hofmann⁵, Erik Strub³, Steven A. Binnie¹, Stefan Heinze⁷, Elmarie Kotze⁸, Chris Du Preez⁸, Stephen G. Tims⁶,

5 Tibor J. Dunai¹

¹Institute of Geology and Mineralogy, University of Cologne, Zùlpicher Str. 49b, 50674 Cologne, Germany.

²Chair of Physical Geography and Geoecology, RWTH Aachen University, Wùllnerstr. 5b, 52062 Aachen, Germany

³Division of Nuclear Chemistry, University of Cologne, Zùlpicher Str. 45, 50674 Cologne, Germany.

⁴Advanced Nuclear Fuels GmbH, Am Seitenkanal 1, 49811 Lingen, Germany.

10 ⁵Institute of Crop Science and Resource Conservation, Soil Science and Soil Ecology, University of Bonn, Nussallee 13, 53115 Bonn, Germany.

⁶Department of Nuclear Physics and Accelerator Applications, Research School of Physics. The Australian National University, Canberra, ACT 2601, Australia

⁷CologneAMS, Institute of Nuclear Physics, University of Cologne, Zùlpicher Str. 77, 50937 Cologne, Germany.

15 ⁸Department of Soil, Crop and Climate Sciences, University of the Free State, P.O. Box 339, Bloemfontein 9300, Republic of South Africa.

Correspondence to: Joel Mohren (joel.mohren@uni-koeln.de)

Abstract. Losses of soil organic matter (SOM) from arable land poses a serious threat to soil fertility and crop yields, and thwarts efforts to conserve soils as carbon sinks to mitigate global warming. Wind erosion can be a major factor in the redistribution of soil fines including SOM, but assessments of its impact have typically been limited by short observation periods of a few years at most. Longer timeframes, extending back to the mid 20th century, may however be probed using the concentrations of radionuclides that were globally distributed by nuclear weapon tests conducted 1950s and early 1960s. The basic concept is that differences in fallout radionuclide (FRN) activities between undisturbed and arable soils can be used to infer soil particle redistribution. In the present work, we have measured activities of ¹³⁷Cs and ²³⁹⁺²⁴⁰Pu in soils from three agricultural regions of the plains of the South African Highveld. The three regions represent distinct agroecosystems and within each region the temporal length of cultivation varies from zero (i.e., native grassland) to almost 100 years. The sampled plots did not show any evidence of fluvial erosion, allowing the contribution of wind erosion to the loss of soil fines, including SOM, to be investigated. For the cultivated soils, radionuclide activities are found to be less than in adjacent native grassland, and the magnitude of the reduction is strongly correlated with the duration of cultivation. Specifically, the original concentrations of both ¹³⁷Cs and ²³⁹⁺²⁴⁰Pu are approximately halved after ~25-45 years of cropping. The initial rate loss relative to the undisturbed soils is, however, considerably higher, with ~6% yr⁻¹ recorded during the first year after native grassland is converted to arable land. We correlate our radionuclide data with previously published SOM contents from the same sampled material and find that the radionuclides are an excellent indicator of SOM decline at the sites we investigate. We conclude that wind erosion can exert a dominant control on SOM loss in arable land of South Africa and by implication at comparable settings on Earth.

1 Introduction

1.1 SOM decline and release of CO₂

The net loss of soil organic matter (SOM) from arable soils poses a serious threat to the fate of human life on Earth. SOM content represents a core soil property, being a key determinant of soil fertility and therefore plant growth (e.g. Palm et al., 2007). Its decline leads to a reduction of crop production yields around the globe, threatening food security (e.g. Bot and Benites, 2005; FAO and ITPS, 2015). The SOM contents in arable soils can be reduced by a variety of factors, including biological, chemical, and physical soil degradation pathways (for an overview see Palm et al., 2007). The threats posed by unsustainable soil management practices, which may be amplified by anthropogenic climate change, have been highlighted in



many studies and summarized in major reports from international organisations (e.g. Reeves, 1997; FAO and ITPS, 2015; 45 FAO, 2017). In particular, aridity has been identified as the most significant factor in the degradation of agricultural land (Prävālie et al., 2021), and unsustainable cropping practices have been shown to affect soil fertility even under more favourable (i.e., less arid) climatic conditions (Smith et al., 2016b). As a consequence, evidence is growing that wind erosion could play an important role in SOM decline, especially in dryland regions, hence affecting both CO₂ budgets and crop yields (as e.g. summarised in FAO and ITPS, 2015).

50 Soil degradation also has a profound effect on the capacity of soils to mitigate global warming by sequestering atmospheric CO₂ (Amelung et al., 2020). In their comprehensive review, Fuss et al. (2018) state that the soils on Earth in their current state could have a technical potential to sequester ~2.3-5.3 Gt CO₂ yr⁻¹ (equivalent to ~0.6 to 1.4 Gt C yr⁻¹). The organic carbon storage in undisturbed soils tends to approach steady state conditions over time, when inputs from net primary productivity and heterotrophic respiration outputs are in balance (Amundson et al., 2015). Presently, however, unsustainable soil cultivation 55 practices have unbalanced soil carbon fluxes on a global scale. Sanderman et al. (2017) approximated the historical carbon debt of humankind against the outer skin of Earth to be already on the order of 116 Gt C (~425 Gt CO₂). Wind erosion contributes significantly to loss of SOC from arable soil, both on regional (e.g. Yan et al., 2005; Chappell et al., 2013) and global scales (Chappell et al., 2019). In particular arable systems on the African continent are considered to be the most heavily affected by degradation on Earth (Prävālie et al., 2021), and degradation by means of wind erosion appears to play a key role 60 in South Africa (Eckardt et al., 2020). The redistribution of soil particles by means of wind can be quantified by dust collectors (e.g. Holmes et al., 2012), but there is a lack of empirical data resolving the fate of SOM over longer timescales (Chappell et al., 2019).

1.2 SOM decline in the South African Highveld grasslands ecoregion

65 A hotspot of cultivation-induced decline of organic matter in arable soils are the arable plains located within the Highveld grasslands ecoregion in the Free State province, Republic of South Africa. Here, various studies have investigated the impact of soil cultivation practices on soil properties under semi-arid (e.g. Lobe et al., 2001; Vos et al., 2020) and temperate (e.g. Lobe et al., 2001; Amelung et al., 2002) climate conditions. Within the Free State province, a huge contribution to land degradation arises from deflation processes, which have been found to be largely a consequence of commercial cropping 70 introduced after the arrival of European settlers (Holmes et al., 2012). In particular surfaces in the semi-arid western portion of the Highveld grasslands have been identified as dust sources, providing fines for more than 70% of all plumes recorded between 2006 and 2016 (Eckardt et al., 2020). Similar scenarios have been identified in other countries around the globe (FAO and ITPS, 2015). The resulting reduction of soil fertility in the Highveld grasslands poses a threat to the food security in the Republic of South Africa. The region contributes significantly to the crop production of the country; about one third of the 75 nation's field crop-cultivated land lies within the Free State administrative boundaries. Consequently, about 40% of maize production, 41% of soybean production, and 20% of wheat production is concentrated in this region (numbers for 2021/22; DALRRD, 2023). The majority of South African soils inherently have low SOM contents, emphasising the important role soil protection plays in South African politics (a comprehensive review on the issue and related studies is given by Du Preez et al., 2019). The low SOM contents of South Africa's soils implies that their potential contribution to the release of SOC as CO₂ 80 per unit area may be limited when compared to other regions on Earth (e.g. Chappell et al., 2019). However, the large spatial extent of surfaces vulnerable to SOC loss in South Africa and comparable settings around the globe increase their significance of potential contribution to the total CO₂ budget. On the plot scale, knowledge on timing and magnitude of SOM content change due to erosional processes but also by aeolian deposition (e.g. Dialynas et al., 2016) is of great importance to further propel efforts to minimise unsustainable cropping practices.



85 In the beginning of the 21st century, Lobe et al. (2001) presented a dataset obtained from three agroecosystems located within
the Highveld grassland ecoregion to investigate the relationship between SOM content in arable sandy soils and the total time
period these soils were cultivated. The agroecosystems were named Harrismith (sample abbreviation HS, mean geographical
centre 28.4°S, 28.9°E), Kroonstad (KR; 27.9°S, 27.0°E), and Tweespruit (TW, 29.2°S, 27.1°E; Fig. 1, Table 1). The
agroecosystem concept provides a frame to group individual sites based on similar soil properties and environmental conditions
90 (cf. du Toit et al., 1994). Besides grouping soil sampling sites, the sampling of Lobe et al. (2001) exclusively focused on flat
($< 3^\circ$) plots, where no traces of fluvial erosion could be ascertained. Furthermore, accurate information on the time periods
over which the sites were subject to cropping was acquired, partially based on preceding studies of du Toit et al. (1994) and
du Preez and du Toit (1995). From splits of the same sample material, consecutive studies analysed amino sugars (Amelung
et al., 2002), lignin compounds (Lobe et al., 2002), SOM ¹³C and ¹⁵N signatures (Lobe et al., 2005), soil aggregates (Lobe et
95 al., 2011), as well as sulphur (Solomon et al., 2005) and phosphorous forms (von Sperber et al., 2017). A key finding of these
studies was that SOM contents decreased exponentially with increasing periods of cultivation. About 65% of SOM was lost
after 90 years of cropping, contemporaneous with a linear decrease of the silt content (2-20 μ m) from about 10% to 5.4%
(mean values; Lobe et al., 2001). Especially for SOC, the exponential decrease with increasing duration of cultivation was
found to be most significant in the silt fraction, providing evidence for a significant contribution of wind erosion to SOM loss
100 (Lobe et al., 2001). Comparable patterns of depletion were observed for amino sugars (Amelung et al., 2002) and oxidised
lignin compounds (Lobe et al., 2002). From $\delta^{13}\text{C}$ analyses in SOM, Lobe et al. (2005) found the relative amount of grassland-
derived SOM to be primarily reduced in the silt fraction, possibly as a consequence of selective silt removal and a relatively
higher input of organic matter from crops, when compared to other grain size fractions. Field evidence of deflation processes
was e.g. reported by Lobe et al. (2011), who observed the accumulation of coarse soil particles close to topographic barriers
105 at some rims of agricultural plots.

1.3 Investigating the contribution of wind erosion to SOM decline in the South African Highveld grasslands ecoregion

As noted above, quantitative information on the impact of wind erosion on the loss of SOM in southern Africa due to cropping
is lacking to date. The means to overcome this problem is provided by fallout radionuclides (FRNs) from the atmospheric
110 nuclear weapons testing in the 1950s and early 1960s. In particular, plutonium isotopes (²³⁹Pu and ²⁴⁰Pu) and caesium-137
(¹³⁷Cs) were distributed world-wide. Both caesium and plutonium are strongly adsorbed on soil fines, including SOM (e.g.
Schimmack et al., 2001; Xu et al., 2013), and plutonium appears not to be taken up significantly by plants in natural settings
(Coughtrey et al., 1984; Harper and Tinnacher, 2008), including grasslands (Little, 1980). Hence, determining the loss of these
isotopes since the atmospheric nuclear testing period allows the quantification of the cultivation-induced loss of soil fines,
115 including SOM. Concentrations of plutonium isotopes in soils can be measured with very high sensitivity using accelerator
mass spectrometry (AMS; e.g. Fifield, 2008), and concentrations of ¹³⁷Cs are determined by low-background γ -ray
spectrometry (e.g. Wallbrink et al., 2003). We use both methods to reveal the contribution of wind erosion to SOM loss in the
three agroecosystems in the South African Highveld initially studied by Lobe et al. (2001) based on splits from original sample
material taken in 1998. The samples encompass a wide range of cultivation histories, ranging from zero (i.e., native grassland)
120 to 98 years. Our approach allows us to investigate the time evolution of SOM loss after native grassland is converted to
cropland. Our study represents one of the first attempts to link plutonium activities to SOM loss by wind in arable lands (cf.
Alewell et al., 2017). Furthermore, we introduce a certain temporal resolution of process rates by analysing arable land with
different cultivation histories.



2 Methods

125 2.1 Background to FRNs and their application to resolve soil particle redistribution

In order to assess soil redistribution, FRN concentrations in undisturbed reference sites are compared with those in adjacent eroding sites (e.g. Schimmack et al., 2002; Zapata, 2002). This approach relies on the assumption of a homogeneous distribution of the target FRN over the limited area covering the undisturbed reference site and the nearby eroding sites. This assumption appears to be valid for most anthropogenic FRNs on a regional scale (e.g. Zapata, 2002). In the northern hemisphere, however, the use of ^{137}Cs in this context has been seriously compromised by additional input from the Chernobyl accident in 1986 [see Meusburger et al. (2020) for a detailed study of $^{239+240}\text{Pu}$ vs ^{137}Cs inventories in Europe] and the Fukushima accident in 2011. The southern hemisphere was not affected, so ^{137}Cs could still be used to complement the measurements of $^{239,240}\text{Pu}$ in the present work. Compared to the plutonium isotopes, ^{137}Cs has a rather short half-life of 30.08 yr [all decay values obtained from the U.S. National Nuclear Data Center (NNDC)]. At the time of measuring (2012), about two thirds of the ^{137}Cs deposited during the atmospheric nuclear weapon tests conducted until the early 1960s had already decayed. Furthermore, the deposition in the southern hemisphere was less than one third of that in the northern hemisphere (UNSCEAR 2000). The concentrations of ^{137}Cs were therefore approaching the detection limit of the γ -counting method, especially in heavily eroded soils and samples from depth. The plutonium isotopes, on the other hand, have much longer half-lives (^{239}Pu : 24,110 yr; ^{240}Pu : 6561 yr), so losses due to decay are minimal. Consequently, plutonium is increasingly supplanting ^{137}Cs as a tracer of soil redistribution (e.g. Alewell et al., 2017). In general, ^{137}Cs and plutonium behave similarly in soils, but evidence is growing that plutonium could have a greater sorption capacity to SOM than ^{137}Cs (e.g. Schimmack et al., 2001; Alewell et al., 2017; Xu et al., 2017). ^{137}Cs has been found to bind more selectively to the clay fraction of soils than does plutonium, implying that ^{137}Cs could be more sensitive to preferential transport than plutonium (Xu et al., 2017). The potential migration pathway of plutonium as a solute is dependent on its oxidation state, but the soil pH values measured (~4.6-6.8; Lobe et al., 2001) rather imply that the least-mobile oxidation state Pu(IV) dominates plutonium inventories at the sites we investigate (cf. Alewell et al., 2017; Meusburger et al., 2020).

2.2 Sampling strategy and sample processing

Since our samples were already taken in 1998 and have been characterised in numerous studies (Lobe et al., 2001; Amelung et al., 2002; Lobe et al., 2002; Lobe et al., 2005; Van Pelt et al., 2007; Lobe et al., 2011), we give here only a brief overview of the sampling strategy that was applied. Following the agroecosystem approach, the sites sampled within an agroecosystem were similar in soil type and environmental conditions (Table 1). Furthermore, sampling focused on agricultural areas with flat surfaces to minimise the possibility of fluvial erosion affecting the SOM content (and FRN concentrations). The sampling sites are located within the present-day local municipalities of Dihlabeng and Maluti a Phofung (HS), Matjhabeng (KR), and Mantsopa (TW). Each of the three datasets includes one composite sample (HS0, KR0, TW0) taken from native grassland sites located adjacent to the respective cultivated sites. At these reference sites, soils had never been subject to ploughing and cropping by the time of sampling. The sites were grazed for up to three months per year by either cattle or sheep at stocking densities of ~0.5 large stock units per ha. At the cultivated sites, most farmers aimed for ploughing depths of 20 cm for cropping. Hence, the ploughing (A_p) horizons of the cultivated soils studied here were mostly 20-30 cm thick, except for two sites in the Harrismith agroecosystem, which were eventually ploughed to a depth of 40 cm (HS30 and HS68). By the time of sampling, none of the sites had ever been irrigated or organically fertilised.

For each site, a radial sampling strategy following the suggestions of Wilding (1985) was applied. Five subsamples were amalgamated per plot to obtain the final sample. Up to nine different agricultural plots were sampled per agroecosystem, with the requirement that the cultivation history (up to 98 yrs) could be precisely ascertained (cf. Lobe, 2003). Sampling focused



165 on topsoils spanning the A_p horizon (0-20 cm). A few samples were also collected at depths of 20-40 cm. The latter were included to test whether the topsoil sampling approach captured most of the plutonium stored within the soil column. The subsamples were taken at a horizontal distance of more than 3 m from each other. Differences in bulk densities between the sites were minor, not correlating with the duration of cropping, and explaining less than 1.3% of the differences in SOC contents between the sites (Lobe et al., 2001). Hence, no equivalent mass corrections were needed for accurate assessments of SOM and Pu loss rates.

The sample preparation for plutonium followed the protocol of Everett (2009). The same protocol was employed for samples processed at the Department of Nuclear Physics, Australia National University (ANU), and the Division of Nuclear Chemistry, University of Cologne (UoC). The physical preparation of the samples was entirely conducted at ANU.

In short, samples were homogenised and the $<20 \mu\text{m}$ fraction separated by sieving. The $<20 \mu\text{m}$ fraction was selected for analysis as representative of the soil fines (cf. Chappell et al., 2013). For AMS, about 20 g of this fraction was dried at 105°C to constant weight. We used this grain size fraction since we expected the majority of $^{239,240}\text{Pu}$ to be adsorbed to the fine soil fractions of the sandy soils we investigated (He and Walling, 1996). After adding a ^{242}Pu spike ($\sim 5 \text{ pg}$, i.e. $\sim 10^{10}$ atoms, diluted from National Institute of Standards and Technology (NIST) Standard Reference Material® 4334H), the samples were dried overnight at 80°C and subsequently ashed at 450°C for 8 h. After ashing, the samples were leached for 48-72 h in 8 M HNO_3 at 90°C . Following the separation of leachate and soil, about 1 g NaNO_2 was added to the leachate to reduce the oxidation state from Pu^{6+} to Pu^{4+} , which is retained by the BioRad AG®-1x8 resin used for the column chromatography ($\sim 3.5 \text{ g}$ resin per column conditioned by 10 ml of 18 M Ω H_2O and 20 ml 8 M HNO_3). After loading the sample solution on to the column, 30 ml of 8 M HNO_3 followed by 70 ml HCl (conc.) were added to elute contaminating elements. Plutonium was then eluted from the columns by adding 25 ml of warm ($\sim 40^\circ\text{C}$), freshly prepared HCl (conc.)/0.1 M NH_4I solution. After taking the eluant to dryness, 2 ml HNO_3 (conc.) and 2 ml HCl (conc.) were added to the samples to remove iodine and NH_4NO_3 . The solution was again taken to dryness at 110°C , and chloride removed by adding another 2 ml of HNO_3 (conc.). In order to provide sufficient bulk material for an AMS sample, 200 μl of a $\text{Fe}(\text{NO}_3)_3$ solution ($\sim 7 \text{ mg Fe g}^{-1}$) was added to the residue and subsequently taken to dryness at 120°C for 24 h or longer. The samples were then baked at 800°C for 8 h to convert the $\text{Fe}(\text{NO}_3)_3$ to Fe_2O_3 , ensuring that the plutonium is uniformly distributed in an iron oxide matrix. In a final step, the samples were mixed with Ag (at ANU) or Nb (at UoC) powder at a ratio of 1:4 by weight and pressed into AMS targets. Replicates were prepared for most of the samples, always in separate batches. The masses of the samples and ^{242}Pu spike are given in Table S2.

As a complement to the plutonium measurements, ^{137}Cs was also measured for selected samples ($n = 12$). From the Harrismith and Kroonstad agroecosystems, two topsoil samples were measured for each (HS0/0-20, HS45/0-20; KR0/0-20, KR40/0-20). The remaining measurements were conducted on topsoil samples (TW0, TW8, TW12, TW32, TW40, TW60, TW90) and one depth sample (TW60/20-40) taken from the Tweespruit agroecosystem. To measure ^{137}Cs , 50-70 g of the same $<20 \mu\text{m}$ material used for AMS were ground to $<10 \mu\text{m}$ using a ring mill and pressed into cylindrical counting discs to ensure a well-defined geometry. The sample processing and measurements were conducted at the Commonwealth Scientific and Industrial Research Organisation, Land and Water Laboratories (CSIRO; Canberra, Australia).

200 2.3 FRN measurements

All FRN measurements presented in this study were conducted in 2012. Initial plutonium measurements ($n = 16$) were conducted at the ANU using the 14UD pelletron tandem accelerator of the Department of Nuclear Physics (Fifield, 2008). The accelerator was operated at $\sim 4 \text{ MV}$, with PuO^+ ions injected. The molecular ions were dissociated and multiple electrons stripped from the plutonium atoms after the first stage of acceleration. This was accomplished by oxygen gas with a thickness of $\sim 0.5 \mu\text{g cm}^{-2}$ confined in an 80 cm long canal in the high-voltage terminal of the accelerator. After the second stage of acceleration, Pu^{5+} ions with an energy of $\sim 24 \text{ MeV}$ were selected by the high-energy analysis system and detected in a gas



ionisation detector with an energy resolution of 3%. At this resolution, plutonium ions are very effectively separated from interfering lower mass ions with the same mass per charge ratio. For example, $^{192}\text{Os}^{4+}$ ions, which would be accepted by the high-energy analysis system, have an energy that is 20% lower than $^{240}\text{Pu}^{5+}$ ions. The $^{239}\text{Pu}/^{242}\text{Pu}$ and $^{240}\text{Pu}/^{242}\text{Pu}$ ratios were measured, allowing the number of ^{239}Pu and ^{240}Pu atoms in the sample and the $^{240}\text{Pu}/^{239}\text{Pu}$ ratio to be deduced. These ratios are also collected in Table S2, along with derived quantities from which the final concentrations are deduced. Quality control was ensured by regular measurements of United Kingdom Atomic Energy Authority (UKAEA) Certified Reference Material (CRM) Pu 5/92138 with ratios $^{240}\text{Pu}/^{242}\text{Pu} = 0.954(2\%)$, $^{239}\text{Pu}/^{242}\text{Pu} = 0.988(2\%)$, and $^{240}\text{Pu}/^{239}\text{Pu} = 0.966(1\%)$. A similar procedure was employed for $n = 47$ measurements at the CologneAMS (Dewald et al., 2013). The 6 MV Tandatron accelerator was operated at 2.9 MV, and ~ 13.6 MeV Pu^{3+} ions were selected after acceleration. A secondary standard, prepared at the Centro Nacional des Aceleradores (CNA, Chamizo et al., 2015) and calibrated against the abovementioned CRM by Christl et al. (2013), was employed. The isotope ratios for this secondary standard are $^{240}\text{Pu}/^{242}\text{Pu} = 0.281(2.1\%)$; $^{239}\text{Pu}/^{242}\text{Pu} = 0.534(2.4\%)$; $^{240}\text{Pu}/^{239}\text{Pu} = 0.530(2.1\%)$. The ^{137}Cs activities of the selected samples were measured by counting the characteristic 662 keV γ -rays. Well-shielded high purity germanium crystals (HPGe; Wallbrink et al., 2003) in the low level counting laboratory of the CSIRO Division of Land and Water (Canberra) were employed. Measuring times ranged between 1 and 9 days per sample.

2.4 Interpretation of $^{239+240}\text{Pu}$ results

Propagated uncertainties provided for individual $^{239+240}\text{Pu}$ concentrations are dominated by AMS counting statistics but include recorded weighing errors. We here report $^{239+240}\text{Pu}$ as activities per mass (here also termed “concentrations” and “specific activities”) of the <20 μm soil fraction, since measures to convert the concentrations into inventories (e.g. grain size distributions, total sample weights, bulk densities) were not comprehensively available (Table S3). However, the low scatter in soil densities of the pooled grassland samples (standard deviation of $0.04\text{--}0.12$ g cm^{-3}) and the available grain size data [partially unpublished, measured by Lobe et al. (2001) and Amelung et al. (2002)] indicate homogenous soil properties across the samples within the respective agroecosystems (Table S1).

In those cases where replicates were measured (predominantly at CologneAMS; HS0/20-40 and HS45/20-40 AMS targets were measured twice at the ANU, here considered as true sample replicates), the quoted plutonium concentrations are weighted means. The corresponding uncertainties are either dominated by internal errors (i.e., dominated by AMS counting statistics) as expressed by the weighted mean error, or by external sources of uncertainty, reflected by the standard error (the larger uncertainty value was chosen for each sample). One outlier was identified in the CologneAMS replicate measurements of TW0/0-20 (TW0/0-20, batch COL-1; Table S2), which we excluded from further interpretation of the data. The measurement was about 70% below the specific activity measured for the other replicates of this sample (TW0/0-20 of batches COL-2 and COL-4, and batch ANU).

3 Results

Table 2 summarises the $^{239+240}\text{Pu}$ and ^{137}Cs concentrations (in mBq kg^{-1}) in the <20 μm fraction of the soils measured in the present work. Sample names, e.g. HS10/0-20, consist of the sample agroecosystem (HS; Harrismith), the years of cultivation (10), and the depth interval sampled in cm (0-20). The raw data from which the plutonium values were derived are given in Table S2. Where multiple measurements were made, the values are weighted means of the individual measurements, and the quoted uncertainties are the larger of the internal and external errors. The internal error is effectively that due to counting statistics, while the external error is the standard deviation of the set of measurements divided by the square root of the number of measurements, i.e. σ/\sqrt{n} . One outlier was identified in the CologneAMS replicate measurements of TW0/0-20



(TW0/0-20, batch COL-1; Table S2). This was excluded from further interpretation of the data. The measurement was about 70% below the concordant measurements for the other three replicates of this sample (TW0/0-20 of batches COL-2 and COL-4, and batch ANU). The blank included into the batch measured at the ANU implied a blank correction of <1% for the samples taken in the top 20 cm of soil. Only for the depth samples TW0/20-40 and TW60/20-40 was the blank subtraction significant, amounting to ~8% and ~4%, respectively. Deviations of CologneAMS and ANU AMS results ($n = 11$ pairs measured in both facilities) are statistically insignificant at a significance level of 0.05 (p-value of 0.95; paired two-tailed t-test). Likewise, replicate measurements at CologneAMS reveal a good reproducibility of the obtained results, with an average error of about 5% with respect to the weighted means calculated for the CologneAMS measurements (one replicate outlier from TW0/0-20 excluded, Sect. 2.4).

3.1 Topsoil ^{239}Pu and ^{240}Pu concentrations in the fraction <20 μm

The measured concentrations in the <20 μm fraction in the top 20 cm of soil span a wide range between $14.5 \pm 0.3 \text{ mBq kg}^{-1}$ (KR98/0-20) and $66.8 \pm 0.9 \text{ mBq kg}^{-1}$ (TW0/0-20). Sample KR98/0-20 is from the plot with the longest cropping history, and the opposite is valid for the pooled native grassland sample TW0/0-20. Similarly, the other samples from the uncultivated plots in the other two agroecosystems also have the concentrations in their respective agroecosystems (HS0/0-20 $56.7 \pm 1.2 \text{ mBq kg}^{-1}$; KR0/0-20 $34.6 \pm 0.7 \text{ mBq kg}^{-1}$).

Figure 2A shows a plot of the measured $^{239+240}\text{Pu}$ concentrations for all three agroecosystems relative to the concentration in the relevant uncultivated plot as a function of the duration of cultivation. A trend of initially decreasing concentration with increasing cropping time is evident, although the rate of decline slows as time goes on. The data may be fitted ($R^2 = 0.77$) to a single exponential plus a constant expression in the form

$$C(t) = C_{eq} + (C_0 - C_{eq})e^{-t/\tau}, \quad (1)$$

where C_0 is the initial concentration (i.e. the uncultivated value; 100% by definition), C_{eq} denotes an equilibrium value, and τ is the time constant for the decline of plutonium with time of cultivation (cf. Lobe et al., 2011). From the fit, C_{eq} equals $52.51 \pm 7.18 \%$ ($1\sigma_x$), and τ equals 8.18 ± 2.93 years.

3.2 Plutonium source and cross-validation with ^{137}Cs

The $^{240}\text{Pu}/^{239}\text{Pu}$ ratios calculated from the atomic ratios of $^{240}\text{Pu}/^{242}\text{Pu}$ and $^{239}\text{Pu}/^{242}\text{Pu}$ measured both at CologneAMS and ANU are internally consistent (Fig. 3). The weighted mean of the measurements for the 0-20 cm samples is 0.180 ± 0.002 . Measured ^{137}Cs activities in the <20 μm fraction (similar to $^{239+240}\text{Pu}$, all ^{137}Cs measurements were performed in 2012) range between $2.04 \pm 0.17 \text{ mBq g}^{-1}$ (TW0/0-20) and $0.40 \pm 0.08 \text{ mBq g}^{-1}$ (KR40/0-20). The ^{137}Cs (A_{Cs}) and $^{239+240}\text{Pu}$ (A_{Pu}) activities correlate linearly ($R^2 = 0.97$; Fig. 4), with

$$A_{Pu} = 0.03A_{Cs} + 0.05. \quad (2)$$

Sample HS0/0-20 has been excluded for the derivation of Eq. (2), as it was identified as an outlier (Sect. 4.1; Table 2). Furthermore, the depth sample TW60/20-40 did not yield meaningful ^{137}Cs data, as the specific activity of ^{137}Cs was below the detection limit of the γ spectrometer. The weighted mean $^{137}\text{Cs}/^{239+240}\text{Pu}$ ratio is 26.69 ± 0.97 (Table S3).

3.3 Plutonium concentrations in depth samples

Ploughing depths in the studied region were usually 20 cm, resulting in the formation of a ploughing horizon A_p of 20-30 cm thickness. In order to investigate whether plutonium could have migrated below this soil layer, samples spanning the depth



interval 20-40 cm were analysed for selected sites from the Tweespruit ($n = 4$) and Harrismith ($n = 2$) agroecosystems. The results are shown in Table 2, and indicate that concentrations are generally much lower than in the top 20 cm, ranging from ~4 to 31% of what is measured in the corresponding topsoil sample (Fig. 5). Sample HS45/20-40 is, however, a conspicuous exception with a surprisingly high activity of 40.9 ± 0.9 mBq kg⁻¹ in the 20-40 cm interval, which is even high than the 26.7 ± 1.2 mBq kg⁻¹ measured in the uppermost 20 cm of the soil (HS45/0-20).

4 Discussion

4.1 FRN concentrations in soil fines of the Highveld ecoregion

295 The ²⁴⁰Pu/²³⁹Pu ratios indicate that plutonium activities measured in soils from the South African Highveld originate predominantly from global fallout. The average ratio of 0.180 ± 0.002 falls comfortably within the range of 0.173 ± 0.014 determined by Kelley et al. (1999) for the southern equatorial (0-30°S) region. Further support for a global fallout origin is provided by the ¹³⁷Cs data. The weighted mean ¹³⁷Cs/²³⁹⁺²⁴⁰Pu ratio of 26.69 ± 0.97 (measured at ~27-30°S) is similar to that measured (24.2 ± 1.3) by Everett et al. (2008) at 18.4°S in the Herbert River catchment in Queensland, Australia. In addition, 300 Bouisset et al. (2018) used data provided by other studies (Hardy et al., 1973; UNSCEAR 2000) as well as their own to calculate a mean ratio ~25 for the southern hemisphere (all cited data decay-corrected to 2012).

In contrast to ¹³⁷Cs, Pu isotopes can be measured on AMS systems with extremely low background (Fifield et al., 1996; Everett et al., 2008; Fifield, 2008). Our plutonium data indicate a high degree of measurement precision, with an average uncertainty attached to the individual samples measured in replicate being below 5%. However, the ¹³⁷Cs measurements can help to further evaluate the ²³⁹⁺²⁴⁰Pu data (Fig. 4). Equation (2) predicts a minor excess of ²³⁹⁺²⁴⁰Pu activities (5.4 ± 1.9 mBq kg⁻¹) in the soil fraction <20 μm as compared to ¹³⁷Cs activity in that fraction. Other studies proposed exceeding ²³⁹⁺²⁴⁰Pu to reflect grain-size dependent preferential adsorption patterns (e.g. Everett et al., 2008; Xu et al., 2017). For our datasets, however, the offset we observe appears to be insignificant given the wide range of other factors that could have influenced the measurements (e.g., background subtraction from the γ-ray measurements). Sample HS0/0-20, i.e. the composite sample of native grasslands in the 310 Harrismith agroecosystem, is the only conspicuous exception to the otherwise linear correlation between ¹³⁷Cs and ²³⁹⁺²⁴⁰Pu concentrations. We cannot offer an explanation for the observation, but note that such deviations are not uncommon in earlier work, with both unexpectedly high and low ¹³⁷Cs activities (e.g. Fulajtar, 2003; Xu et al., 2013; Bouisset et al., 2018). In general, the linear correlation between ¹³⁷Cs and ²³⁹⁺²⁴⁰Pu activities supports the assumption that chemical erosion does not contribute to the loss of the FRNs in the soils we investigate (cf. Everett et al., 2008).

315

4.2 The fate of ²³⁹⁺²⁴⁰Pu in topsoil fines after native grassland is converted to arable land

In most undisturbed soils, the majority of the plutonium originating from global fallout is stored in the uppermost centimetres of the soil column (e.g. Hoo et al., 2011; Alewell et al., 2017; Lal et al., 2020). The small amount of plutonium in the 20-40 cm depth interval for the uncultivated HS0 and TW0 samples would indicate the same is true within the agroecosystems we 320 investigate. The plutonium concentrations we measure in our samples from native grassland represent upper limits for ²³⁹⁺²⁴⁰Pu within the respective agroecosystems. Hence, these samples can be used as reference to assess the decline of plutonium concentrations in adjacent, cultivated plots over time relative to the reference sites.

In the cultivated soils, however, ploughing will distribute the plutonium-marked soil particles across the ~20 cm ploughing horizon (e.g. Fulajtar, 2003). With the exception of the anomalous HS45/20-40 sample (see sect. 3.3), the plutonium 325 concentrations measured from the depth samples generally support the conclusion that the majority of ²³⁹⁺²⁴⁰Pu was indeed stored in the upper 20 cm of the soil columns by the time of sampling (Fig. 5). It is noteworthy that HS45 is one of two samples



where the bulk density of the depth sample was lower than the bulk density of the corresponding topsoil sample (1.24 g cm^{-3} vs. 1.31 g cm^{-3} ; Table S1). In addition, Harrismith is the only agroecosystem where also ploughing to 40 cm depth had been reported, although not recorded by us for this specific sample. Bioturbation can result in a further relocation of topsoil particles to depths exceeding the A_p horizon, but overall activities would be expected to decrease rather than increase with depth (Fulajtar, 2003). Since our sampling strategy included a spatial averaging of sampling material from each plot investigated (Sect. 2.2), the best explanation for the elevated plutonium activity in HS45/20-40 may be related to a former ploughing to 40 cm that was not recorded during farmers' interviews or to sample contamination. However, we also note that such patterns of increasing FRN activities in deeper profile sections of ploughed soil horizons have been measured by Van Pelt et al. (2007), who comprehensively investigated the application of ^{137}Cs to quantify wind erosion of Aridic Paleustalfs. Assuming that climatic conditions and cropping practices (the ploughing depth and cropped plant species variety did not change over time) remained reasonably steady during the second half of the 20th century, the plutonium data indicate that the greatest loss of soil fines occurs during the first years after the conversion from native grassland to arable land. Equation (1) predicts a decline in the $^{239+240}\text{Pu}$ concentration of ~6% to ~2% per year during the first 10 years of cropping. After ~25-45 years, the measured concentrations approach an equilibrium level at about 50-60% of the initial reference values, i.e. Eq. (1) predicts that about half of the initial specific activities in the fine fraction is retained over the long term. The finding of an exponential decline over time towards the equilibrium asymptote indicates that a certain fraction of plutonium adsorbs to soil fines that appear to be shielded against wind erosion. The reason for this pattern could be linked to soil aggregation. For the sites we investigated, Lobe et al. (2011) found an equilibrium soil content of more than 60% for aggregates $>250 \mu\text{m}$ after ~17-31 years of cropping. Such particle sizes are not likely to be suspended by wind action, achieving a certain level of protection for aggregated fines. The change in the distribution of soil aggregate fractions within the soils was generally found to have approached an equilibrium after ~31 years of cropping, mimicking the fate of $^{239+240}\text{Pu}$ concentrations (Lobe et al., 2011). However, aggregation was shown to be least developed in the Kroonstad agroecosystem due to a greater abundance of coarse-grained particles (soil types defined as loamy sand, Lobe et al., 2011; see also Table S1). In this agroecosystem, our related plutonium concentrations in the fraction $<20 \mu\text{m}$ do often significantly exceed the trend predicted by the exponential model (Fig. 2A), indicating that other mechanisms could be at play affecting the primarily wind-governed decrease of $^{239+240}\text{Pu}$ in arable land over time, some of which we discuss below.

4.3 Temporal limitation of $^{239+240}\text{Pu}$ topsoil concentrations

The plutonium isotopes measured in this study allow us to reconstruct the fate of soil fines after native grassland is converted to arable land in the South African Highveld. However, the approach has a temporal limitation inherent to the application of anthropogenic FRNs for tracing the redistribution of soil particles. Since fallout occurred as consequence of atmospheric nuclear weapon tests, the timescales we can resolve is on its lower end limited by the major episode these tests were conducted, i.e. the mid 1950s to early 1960s (UNSCEAR 2000). Arable land that has been subject to ploughing before that time (we use the year 1963 as anchor point, i.e. the year the fallout of FRNs peaked on the southern hemisphere, UNSCEAR 2000) is very likely to have faced erosion before the FRNs were deposited. The $^{239+240}\text{Pu}$ activities obtained from arable land with a cultivation history exceeding 35 years mostly plots below the equilibrium asymptote defined by Eq. (1) in Fig. 2A, i.e. the weighted mean of these data points is $36.9 \pm 3.2\%$ (arithmetic mean $43.9 \pm 9.7\%$). The low scatter of these points is noteworthy because apart from the possibility of varying environmental conditions prevailing even across short spatial distances (e.g. Smith et al., 2016a), other factors appear to be realistic that potentially could have significantly affected the deposition of fallout nuclides on the sites we investigated. For example, plutonium was deposited during the 1950s and 1960s on soils that by that time had been already subject to cultivation practices for decades. Consequently, soil properties at these sites had been already altered, with SOM contents being decreased (Fig. 2B) and/or soil texture significantly changed. Another possible factor



that may lower plutonium concentrations in the >35 years old plots is linked to fallout interception by plants. Adsorption of
370 FRNs on plant surfaces, including crops, has been found to be potentially significant (e.g. Reissig, 1965; Nakanishi, 2013),
and thus a certain proportion of the introduced plutonium could have been lost during crop harvest during the early 1960s.
Occasional grazing may also have contributed to a loss of FRNs, but given the low stocking densities more likely due to the
ingestion of fallout-exposed grass (cf. Sato et al., 2017) than by means of wind erosion. These mechanisms may explain the
minor trend of dropping $^{239+240}\text{Pu}$ concentrations in some plots exceeding 35 years of cultivation. However, in general terms
375 the soil retention capabilities with respect to $^{239+240}\text{Pu}$ adsorption appear to have been similar in native grasslands and more
degraded cultivated soils by the time of FRN deposition. Another possibility factor affecting the overall decline of plutonium
concentration over the long term could be related to influx of Pu-marked soil fines to the investigated sites (Sect. 4.5).

4.4 Adsorption of $^{239+240}\text{Pu}$ to SOM and deflation of SOM

380 Despite the temporal limitation inherent to the application of FRNs, it is evident that $^{239+240}\text{Pu}$ concentrations and SOM contents
behave similar after native grassland has been converted to arable land. Similar to $^{239+240}\text{Pu}$, SOC in the fraction <20 μm has
been shown to approach an equilibrium concentration of ~47-48% of the initial values after about 53-55 years of cropping,
with $\tau = 11.1$ years (Fig. 2B; Lobe et al., 2001; their exponential model). The difference in time constants might indicate that
the plutonium was not uniformly distributed throughout the 20 cm but more concentrated towards the surface after initial
385 ploughing, and hence was preferentially lost due to wind erosion during the first year(s) after native grassland was converted
to arable land [cf. Scanlan and Davies (2019) for an assessment of soil mixing efficiencies of different tillage treatments].
However, SOM contents and Pu concentrations both reflect largest rates of decline during the first years after native grasslands
were converted to arable land. The similar behaviour of $^{239+240}\text{Pu}$ activities and SOM content over time indicates a strong
linkage between both variables. This relationship is underscored by high correlation coefficients ($R^2 = 0.64$ to 0.79 ; Fig. 2C)
390 between the plutonium concentrations (1963-1998) and SOC contents in the clay and silt fractions as measured by Lobe et al.
(2001) (Table S4). Similar R^2 values ($0.64 - 0.93$) are obtained when $^{239+240}\text{Pu}$ is correlated to total N contents (Fig. S1).
Lobe et al. (2001) identified the turnover of SOM in the silt and clay fractions as the main factor controlling the time-dependent
decrease of SOM stocks in the investigated arable soils. Mineralisation processes were believed to play an important role for
the overall SOM decline, as expressed by the approach of lower SOM equilibrium levels (e.g. du Toit et al., 1994; du Preez
395 and du Toit, 1995; Lobe et al., 2001; Lobe et al., 2002). The approach of a time-independent SOM equilibrium has been
attributed to the mineralisation-driven depletion of the labile SOM pool, thereby increasing relative dominance of the stable
SOM pool in the soils (Lobe et al., 2001). Another contribution to the SOM decline was assumed to be caused by a strongly
reduced input of organic matter during the fallow (Lobe et al., 2001; Amelung et al., 2002; Lobe et al., 2002), as well as due
to the loss of silts via wind erosion, which likely also contained old oxidised lignin (Lobe et al., 2001; Lobe et al., 2002). Here,
400 we indeed observe a strong correlation between plutonium concentrations and SOM contents in the <20 μm fraction of the
soils. Hence, we find it reasonable to assume that $^{239+240}\text{Pu}$ is not likely to reflect a dominance of mineralisation processes but
that SOM contents are primarily also affected by deflation processes rather than turnover rates. This finding is in line with
similar studies who highlighted the significance of SOC removal due to wind erosion on different spatial scales (e.g. Yan et
al., 2005; Chappell et al., 2013; Chappell et al., 2019). At least, losses of old SOM <20 μm seem to be largely controlled by
405 wind erosion processes.

It should be noted that the close correlation between the <20 μm SOM loss and Pu concentration decrease is unlikely to solely
explain the loss of bulk SOM by erosion, since large parts of SOM losses were also due to particulate organic matter (POM),
which by definition occurred in a size range excluded for Pu analyses. Yet, also POM may be blown away to a certain degree.
Besides, the fate of mineral associated organic matter and POM can be closely coupled (Lobe et al., 2001; Sokol et al., 2019;
410 Lavallee et al., 2020), and there was only very little formation of new SOM from the crops (Lobe et al., 2005). Consequently,



wind erosion may have altered internal steady-state equilibria that control the partitioning of SOC between POM and mineral surfaces (cf. Lützow et al., 2006; Cotrufo and Lavalée, 2022). With the latter being lost by erosion, possibly also the pressure on POM degradation increased, particularly if POM was to some extent protected by minerals.

This hypothesis could thus be to a certain extent modified by considering soil aggregation (Sect. 4.2). Breaking down soil aggregates as a consequence of ploughing could make SOM available for decay which would otherwise be more resistant to chemical oxidation (Elliott, 1986). While we do not assume that $^{239+240}\text{Pu}$ concentrations will reflect this mineralisation mechanism directly, the supply of soil fines to be carried away by wind erosion could mimic the mineralisation loss rate of previously protected SOM. This mechanism, together with the linear decrease of silt contents (no trend observable for the clay fraction) in cropped plots as observed by Lobe et al. (2001) (Fig. S2), may imply that $^{239+240}\text{Pu}$ activities will not approach an equilibrium in plots older than 35 years as predicted by Eq. (1). Instead, a bi-exponential model as suggested to predict SOM decrease over time (e.g. Lobe et al., 2001; Amelung et al., 2002; Lobe et al., 2011) could reflect the long-term fate of $^{239+240}\text{Pu}$ concentrations more accurately, even despite the fact that our analyses neglected the soil fraction $>20\ \mu\text{m}$. To resolve this issue, longer timescales need to be monitored in future studies.

A further mechanism that could be influencing SOM contents and absolute Pu activities may be related to deposition processes (cf. Chappell et al., 2014). Eckardt et al. (2020) concluded that the vast majority of dust plumes in South Africa have trajectories towards the southeast, approaching the Indian Ocean. In our study, we measure the highest activities in the downwind sites. The composite grassland sample HS0/0-20 has an activity twice as high as the most north-west located sites (KR0/0-20), generally coinciding with SOM patterns as published by Lobe et al. (2001). This pattern is further reflected by grain size data, indicating that KR soils had the lowest clay and silt fraction of all soils (Fig. S2) by the time of sampling. Such differences between the three agroecosystems may not only be attributed to slightly differing soil properties (Table 1, S4) but to regional environmental conditions and atmospheric circulation patterns (distance between the agroecosystems is about 100-300 km), as found elsewhere (e.g. Funk et al., 2011; Xu et al., 2017; Meusburger et al., 2020).

4.5 Implications for land management practices and carbon budgets

Although certain mechanisms may limit the effect of wind erosion on SOM decline over time, wheat and maize yields have been reported to be more than halved after about 30 years of cropping at the sites we investigated (Lobe et al., 2005). The severity of wind erosion is very likely to be strongly promoted by the cropping practices that are commonly observed in the Free State province (Eckardt et al., 2020) and that were applied at the sites we investigated at least until the time of sampling. These cropping practices include the clearance of arable land from any vegetation for up to 6 months per crop rotation cycle (1-2 years) to minimise soil water loss by plant uptake during the dry season. Consequently, dust emissions peak during the winter months, when arable soils remain largely unprotected in South Africa's rainfed agriculture (Eckardt et al., 2020). The data we present provides further evidence that these cropping practices cannot be termed sustainable. We find similar patterns of relative SOM decline in our investigated sites which are located in different agroecosystems at distances of hundreds of kilometres between each other. Based on the observations of Eckardt et al. (2020), it appears reasonable to assume that SOM particles are conveyed to the Pacific Ocean. It is still a matter of debate whether oceans can be generally considered as sinks for organic carbon (for an overview see Chappell et al., 2019), but it seems likely that SOC particles' exposition to decay is enhanced during transport in the atmosphere (e.g. Lal, 2006), contributing to negatively balance the worldwide carbon budgets. However, the effects may be less severe than they would have been if mineralisation controlled the release of CO_2 , given the chance of carbon fixation in the ocean.

450



5 Conclusion

We have measured fallout radionuclides (^{137}Cs , $^{239+240}\text{Pu}$) to quantitatively investigate the linkages between SOM decline and wind erosion in plain arable land of South Africa's Highveld grassland ecoregion. Wind erosion, a physical process, appears to be a dominant factor removing SOM as particles from the plots. Under the impression of anthropogenic climate change, which is in turn predicted to increase both drought and storm event probabilities southern Africa (Arias et al., 2021), our time-integrated FRN data records the effects of unsustainable cropping practices in the South African Highveld ecoregion. Furthermore, it underlines the necessity to consider wind erosion of SOC for CO_2 release estimations.

Author contribution

JM – Formal analysis, validation, visualisation, writing – original draft, writing – review and editing; HW – Formal analysis, investigation, validation, visualisation, writing – original draft; WA – Conceptualisation, funding acquisition, project administration, resources, supervision, writing – review and editing; LKF - Formal analysis, investigation, methodology, project administration, resources, supervision, validation, writing – review and editing; ASH – Project administration, resources, supervision, writing – review and editing; ES – Conceptualisation, methodology, project administration, resources, supervision, writing – review and editing; SAB – Project administration, resources, supervision; SH – Investigation, methodology, resources; EK – Investigation, resources; CDP – Investigation, resources, writing – review and editing; SGT – Investigation, methodology, resources, supervision; TJD – Conceptualisation, funding acquisition, project administration, resources, supervision, writing – review and editing.

470 Competing interests

The authors declare that they have no conflict of interest.

Acknowledgements

This work was funded by the Deutsche Forschungsgemeinschaft (German Research Foundation, DFG) in the frame of TRR228 (project A01). Claus Feuerstein is thanked for his successful efforts to improve the plutonium measurement capabilities at CologneAMS. Wulf Amelung additionally acknowledges support from the DFG under Germany's Excellence Strategy, EXC-2070-390732324-PhenoRob. The Heavy Ion Accelerator Facility (HIAF) at ANU is supported by the National Collaborative Research Infrastructure Strategy (NCRIS) of the Australian Government.

480

485



References

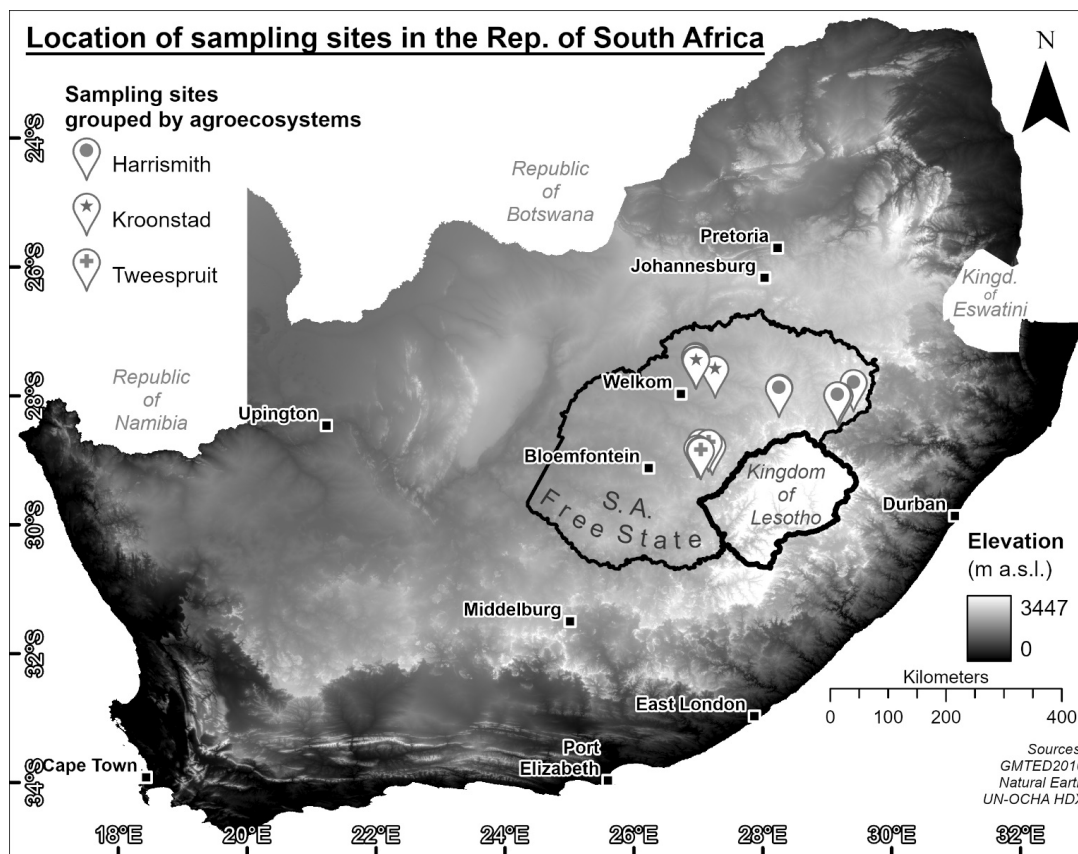
- Alewell, C., Pitois, A., Meusburger, K., Ketterer, M., and Mabit, L.: ²³⁹⁺²⁴⁰Pu from “contaminant” to soil erosion tracer: Where do we stand?, *Earth-Science Reviews*, 172, 107-123, 2017.
- 490 Amelung, W., Lobe, I., and Du Preez, C. C.: Fate of microbial residues in sandy soils of the South African Highveld as influenced by prolonged arable cropping, *European Journal of Soil Science*, 53, 29-35, 2002.
- Amelung, W., Bossio, D., de Vries, W., Kogel-Knabner, I., Lehmann, J., Amundson, R., Bol, R., Collins, C., Lal, R., Leifeld, J., Minasny, B., Pan, G., Paustian, K., Rumpel, C., Sanderman, J., van Groenigen, J. W., Mooney, S., van Wesemael, B., Wander, M., and Chabbi, A.: Towards a global-scale soil climate mitigation strategy, *Nat Commun*, 11, 5427, 2020.
- 495 Amundson, R., Berhe, A. A., Hoppmans, J. W., Olson, C., Szein, A. E., and Sparks, D. L.: Soil science. Soil and human security in the 21st century, *Science*, 348, 1261071, 2015.
- Arias, P., Bellouin, N., Coppola, E., Jones, R., Krinner, G., Marotzke, J., Naik, V., Palmer, M., Plattner, G.-K., Rogelj, J., Rojas, M., Sillmann, J., Storelvmo, T., Thorne, P., Trewin, B., Rao, K., Adhikary, B., Allan, R., Armour, K., and Zickfeld, K.: IPCC AR6 WGI Technical Summary. In: *Climate Change 2021: The Physical Science Basis. Contribution of Working Group I to the Sixth Assessment Report of the Intergovernmental Panel on Climate Change*, V. Masson-Delmotte, P. Zhai, A. Pirani, S. L. Connors, C. Péan, S. Berger, N. Caud, Y. Chen, L. Goldfarb, M. I. Gomis, M. Huang, K. Leitzell, E. Lonnoy, J. B. R. Matthews, T. K. Maycock, T. Waterfield, O. Yelekçi, R. Yu, and Zhou, B. (Eds.), Cambridge University Press, United Kingdom and New York, NY, USA, 2021.
- 500 Beck, H. E., Zimmermann, N. E., McVicar, T. R., Vergopolan, N., Berg, A., and Wood, E. F.: Present and future Köppen-Geiger climate classification maps at 1-km resolution, *Scientific Data*, 5, 180214, 2018.
- Bot, A. and Benites, J.: The importance of soil organic matter: Key to drought-resistant soil and sustained food production. In: *FAO Soils Bulletin, Food and Agriculture Organization of the United Nations (FAO)*, 2005.
- Bouisset, P., Nohl, M., Bouville, A., and Leclerc, G.: Inventory and vertical distribution of ¹³⁷Cs, ²³⁹⁺²⁴⁰Pu and ²³⁸Pu in soil from Raivavae and Hiva Oa, two French Polynesian islands in the southern hemisphere, *Journal of Environmental Radioactivity*, 183, 82-93, 2018.
- 510 Boulyga, S. F. and Becker, J. S.: Isotopic analysis of uranium and plutonium using ICP-MS and estimation of burn-up of spent uranium in contaminated environmental samples, *Journal of Analytical Atomic Spectrometry*, 17, 1143-1147, 2002.
- Chamizo, E., López-Lora, M., Villa, M., Casacuberta, N., López-Gutiérrez, J. M., and Pham, M. K.: Analysis of ²³⁶U and plutonium isotopes, ^{239,240}Pu, on the 1MV AMS system at the Centro Nacional de Aceleradores, as a potential tool in oceanography, *Nuclear Instruments and Methods in Physics Research Section B: Beam Interactions with Materials and Atoms*, 361, 535-540, 2015.
- 515 Chappell, A., Webb, N. P., Butler, H. J., Strong, C. L., McTainsh, G. H., Leys, J. F., and Viscarra Rossel, R. A.: Soil organic carbon dust emission: an omitted global source of atmospheric CO₂, *Glob Chang Biol*, 19, 3238-3244, 2013.
- Chappell, A., Webb, N. P., Viscarra Rossel, R. A., and Bui, E.: Australian net (1950s–1990) soil organic carbon erosion: implications for CO₂ and land–atmosphere modelling, *Biogeosciences*, 11, 5235-5244, 2014.
- 520 Chappell, A., Webb, N. P., Leys, J. F., Waters, C. M., and Eyres, M. J.: Minimising soil organic carbon erosion by wind is critical for land degradation neutrality, *Environmental Science & Policy*, 93, 43-52, 2019.
- Christl, M., Vockenhuber, C., Kubik, P. W., Wacker, L., Lachner, J., Alfimov, V., and Synal, H. A.: The ETH Zurich AMS facilities: Performance parameters and reference materials, *Nuclear Instruments and Methods in Physics Research Section B: Beam Interactions with Materials and Atoms*, 294, 29-38, 2013.
- 525 Cotrufo, M. F. and Lavelle, J. M.: Chapter One - Soil organic matter formation, persistence, and functioning: A synthesis of current understanding to inform its conservation and regeneration. In: *Advances in Agronomy*, Sparks, D. L. (Ed.), Academic Press, 2022.
- Coughtrey, P., Jackson, D., Jones, C., Kane, P., and Thorne, M.: Radionuclide distribution and transport in terrestrial and aquatic ecosystems. A critical review of data. Volume 4, A. A. Balkema, Rotterdam, 1984.
- 530 Department of Agriculture, Land Reform & Rural Development (DALRRD): Abstract of Agricultural Statistics 2023. Directorate Statistics and Economic Analysis, Pretoria, 2023.
- Dewald, A., Heinze, S., Jolie, J., Zilges, A., Dunai, T., Rethemeyer, J., Melles, M., Staubwasser, M., Kuczewski, B., Richter, J., Radtke, U., von Blanckenburg, F., and Klein, M.: CologneAMS, a dedicated center for accelerator mass spectrometry in Germany, *Nuclear Instruments and Methods in Physics Research Section B: Beam Interactions with Materials and Atoms*, 294, 18-23, 2013.
- 535 Dialynas, Y. G., Bastola, S., Bras, R. L., Billings, S. A., Markewitz, D., and Richter, D. d.: Topographic variability and the influence of soil erosion on the carbon cycle, *Global Biogeochemical Cycles*, 30, 644-660, 2016.
- du Preez, C. C. and du Toit, M. E.: Effect of cultivation on the nitrogen fertility of selected agro-ecosystems in South Africa, *Fertilizer Research*, 42, 27-32, 1995.
- Du Preez, C. C., van Huyssteen, C. W., and Amelung, W.: Changes in soil organic matter content and quality in South African arable land. In: *Soil degradation and restoration in Africa*, CRC press, 2019.
- 540 du Toit, M. E., du Preez, C. C., Hensley, M., and Bennie, A. T. P.: Effek van bewerking op die organiese materiaalinhoud van geselekteerde droëlandgronde in Suid-Afrika, *South African Journal of Plant and Soil*, 11, 71-79, 1994.
- Eckardt, F. D., Bekiswa, S., Von Holdt, J. R., Jack, C., Kuhn, N. J., Mogane, F., Murray, J. E., Ndara, N., and Palmer, A. R.: South Africa’s agricultural dust sources and events from MSG SEVIRI, *Aeolian Research*, 47, 100637, 2020.
- 545 Elliott, E. T.: Aggregate Structure and Carbon, Nitrogen, and Phosphorus in Native and Cultivated Soils, *Soil Science Society of America Journal*, 50, 627-633, 1986.
- Everett, S. E., Tims, S. G., Hancock, G. J., Bartley, R., and Fifield, L. K.: Comparison of Pu and ¹³⁷Cs as tracers of soil and sediment transport in a terrestrial environment, *Journal of Environmental Radioactivity*, 99, 383-393, 2008.
- Everett, S. E.: Assessment of plutonium as a tracer of soil and sediment transport using accelerator mass spectrometry, Dissertation, Australian National University, XXII, 165 pp., 2009.
- 550 FAO and ITPS: Status of the World’s Soil Resources (SWRS) – Main Report., Food and Agriculture Organization of the United Nations and Intergovernmental Technical Panel on Soils, Rome, Italy, 2015.
- FAO: Soil Organic Carbon: the hidden potential, Food and Agriculture Organization of the United Nations, Rome, Italy, 2017.
- 555 Fifield, L. K., Cresswell, R. G., di Tada, M. L., Ophel, T. R., Day, J. P., Clacher, A. P., King, S. J., and Priest, N. D.: Accelerator mass spectrometry of plutonium isotopes, *Nuclear Instruments and Methods in Physics Research Section B: Beam Interactions with Materials and Atoms*, 117, 295-303, 1996.



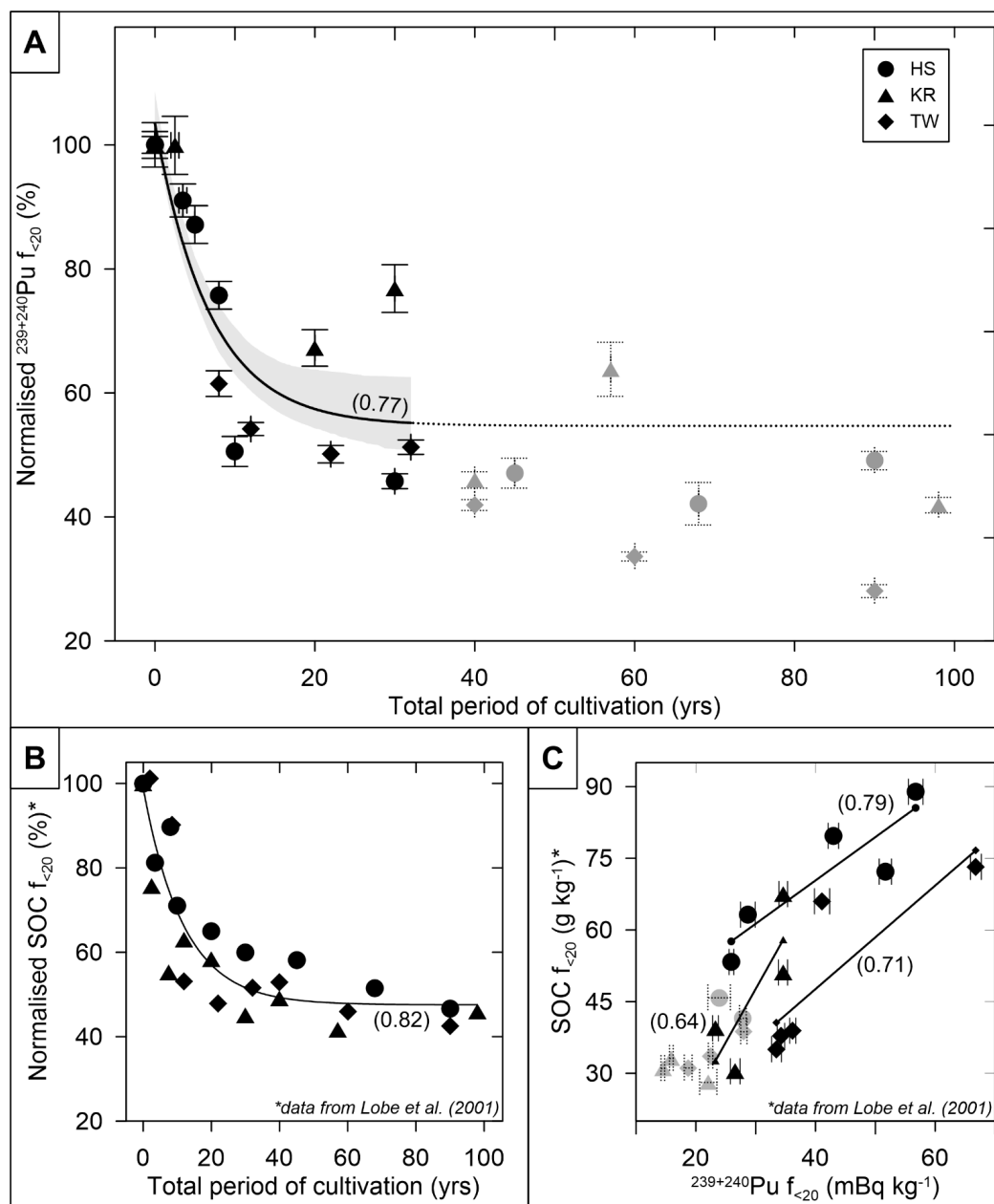
- Fifield, L. K.: Accelerator mass spectrometry of the actinides, *Quaternary Geochronology*, 3, 276-290, 2008.
- Fulajtar, E.: Assessment of soil erosion on arable land using ^{137}Cs measurements: a case study from Jaslovske Bohunice, Slovakia, *Soil and Tillage Research*, 69, 139-152, 2003.
- 560 Funk, R., Li, Y., Hoffmann, C., Reiche, M., Zhang, Z., Li, J., and Sommer, M.: Using ^{137}Cs to estimate wind erosion and dust deposition on grassland in Inner Mongolia-selection of a reference site and description of the temporal variability, *Plant and Soil*, 351, 293-307, 2011.
- Fuss, S., Lamb, W. F., Callaghan, M. W., Hilaire, J., Creutzig, F., Amann, T., Beringer, T., de Oliveira Garcia, W., Hartmann, J., Khanna, T., Luderer, G., Nemet, G. F., Rogelj, J., Smith, P., Vicente, J. L. V., Wilcox, J., del Mar Zamora Dominguez, M., and Minx, J. C.: Negative emissions—Part 2: Costs, potentials and side effects, *Environmental Research Letters*, 13, 2018.
- 565 Hardy, E. P., Krey, P. W., and Volchok, H. L.: Global Inventory and Distribution of Fallout Plutonium, *Nature*, 241, 444-445, 1973.
- Harper, R. M. and Tinnacher, R. M.: Plutonium. In: *Encyclopedia of Ecology*, Jørgensen, S. E. and Fath, B. D. (Eds.), Academic Press, Oxford, 2008.
- He, Q. and Walling, D. E.: Interpreting particle size effects in the adsorption of ^{137}Cs and unsupported ^{210}Pb by mineral soils and sediments, *Journal of Environmental Radioactivity*, 30, 117-137, 1996.
- 570 Holmes, P. J., Thomas, D. S. G., Bateman, M. D., Wiggs, G. F. S., and Rabumbulu, M.: EVIDENCE FOR LAND DEGRADATION FROM AEOLIAN SEDIMENT IN THE WEST-CENTRAL FREE STATE PROVINCE, SOUTH AFRICA, *Land Degradation & Development*, 23, 601-610, 2012.
- Hoo, W. T., Fifield, L. K., Tims, S. G., Fujioka, T., and Mueller, N.: Using fallout plutonium as a probe for erosion assessment, *Journal of Environmental Radioactivity*, 102, 937-942, 2011.
- 575 IUSS Working Group WRB: World Reference Base for Soil Resources 2014, update 2015. International soil classification system for naming soils and creating legends for soil maps, FAO, Rome, 2015.
- Kelley, J. M., Bond, L. A., and Beasley, T. M.: Global distribution of Pu isotopes and ^{237}Np , *Science of The Total Environment*, 237-238, 483-500, 1999.
- 580 Krey, P., Hardy, E., Pachucki, C., Rourke, F., Coluzza, J., and Benson, W.: Mass isotopic composition of global fall-out plutonium in soil, 1976.
- Lal, R.: Influence of Soil Erosion on Carbon Dynamics in the World. In: *Soil erosion and carbon dynamics*, Roose, E. J., Lal, R., Feller, C., Barthès, B., and Stewart, B. A. (Eds.), Advances in soil science, CRC Press, Boca Raton, 2006.
- Lal, R., Fifield, L. K., Tims, S. G., Wasson, R. J., and Howe, D.: A study of soil erosion rates using (^{239}Pu), in the wet-dry tropics of northern Australia, *J Environ Radioact*, 211, 106085, 2020.
- 585 Lavallee, J. M., Soong, J. L., and Cotrufo, M. F.: Conceptualizing soil organic matter into particulate and mineral-associated forms to address global change in the 21st century, *Glob Chang Biol*, 26, 261-273, 2020.
- Little, C. A.: Plutonium in a grassland ecosystem. In: *Transuranic elements in the environment*, US Department of Energy Washington, DC, 1980.
- 590 Lobe, I., Amelung, W., and Du Preez, C. C.: Losses of carbon and nitrogen with prolonged arable cropping from sandy soils of the South African Highveld, *European Journal of Soil Science*, 52, 93-101, 2001.
- Lobe, I., Du Preez, C. C., and Amelung, W.: Influence of prolonged arable cropping on lignin compounds in sandy soils of the South African Highveld, *European Journal of Soil Science*, 53, 553-562, 2002.
- Lobe, I.: Fate of organic matter in sandy soils of the South African Highveld as influenced by the duration of arable cropping, *Lehrstuhl für Bodenkunde und Bodengeographie der Univ. Bayreuth, Bayreuth*, 2003.
- 595 Lobe, I., Bol, R., Ludwig, B., Du Preez, C. C., and Amelung, W.: Savanna-derived organic matter remaining in arable soils of the South African Highveld long-term mixed cropping: Evidence from ^{13}C and ^{15}N natural abundance, *Soil Biology and Biochemistry*, 37, 1898-1909, 2005.
- Lobe, I., Sandhage-Hofmann, A., Brodowski, S., du Preez, C. C., and Amelung, W.: Aggregate dynamics and associated soil organic matter contents as influenced by prolonged arable cropping in the South African Highveld, *Geoderma*, 162, 251-259, 2011.
- 600 Lützw, M. v., Kögel-Knabner, I., Ekschmitt, K., Matzner, E., Guggenberger, G., Marschner, B., and Flessa, H.: Stabilization of organic matter in temperate soils: mechanisms and their relevance under different soil conditions – a review, *European Journal of Soil Science*, 57, 426-445, 2006.
- Meusburger, K., Evrard, O., Alewell, C., Borrelli, P., Cinelli, G., Ketterer, M., Mabit, L., Panagos, P., van Oost, K., and Ballabio, C.: Plutonium aided reconstruction of caesium atmospheric fallout in European topsoils, *Sci Rep*, 10, 11858, 2020.
- 605 Nakanishi, T. M.: The Overview of Our Research. In: *Agricultural Implications of the Fukushima Nuclear Accident*, Nakanishi, T. M. and Tanoi, K. (Eds.), Springer Japan, Tokyo, 2013.
- National Institution of Standards and Technology (NIST): Standard Reference Material®4334I Plutonium-242 Radioactivity Standard. 2010. National Nuclear Data Center (NNDC): <https://www.nndc.bnl.gov/nudat3/>, last access: 10.01.2022.
- 610 Palm, C., Sanchez, P., Ahamed, S., and Awiti, A.: Soils: A Contemporary Perspective, *Annual Review of Environment and Resources*, 32, 99-129, 2007.
- Prăvălie, R., Patriche, C., Borrelli, P., Panagos, P., Roșca, B., Dumitrașcu, M., Nita, I.-A., Săvulescu, I., Birsan, M.-V., and Bandoc, G.: Arable lands under the pressure of multiple land degradation processes. A global perspective, *Environmental Research*, 194, 110697, 2021.
- 615 Reeves, D. W.: The role of soil organic matter in maintaining soil quality in continuous cropping systems, *Soil and Tillage Research*, 43, 131-167, 1997.
- Reissig, H.: ^{137}Cs in landwirtschaftlichen Nutzpflanzen und Böden auf dem Territorium der DDR 1960–1963, *Archives of Agronomy and Soil Science*, 9, 955-972, 1965.
- Sanderman, J., Hengl, T., and Fiske, G. J.: Soil carbon debt of 12,000 years of human land use, *Proc Natl Acad Sci U S A*, 114, 9575-9580, 2017.
- 620 Sato, I., Sasaki, J., Satoh, H., Murata, T., Otani, K., and Okada, K.: Radioactive cesium and potassium in cattle living in the 'zone in preparation for the lifting of the evacuation order' of the Fukushima nuclear accident, *Anim Sci J*, 88, 1021-1026, 2017.
- Scanlan, C. A. and Davies, S. L.: Soil mixing and redistribution by strategic deep tillage in a sandy soil, *Soil and Tillage Research*, 185, 139-145, 2019.
- 625 Schimmack, W., Auerswald, K., and Bunzl, K.: Can $^{239+240}\text{Pu}$ replace ^{137}Cs as an erosion tracer in agricultural landscapes contaminated with Chernobyl fallout?, *Journal of Environmental Radioactivity*, 53, 41-57, 2001.
- Schimmack, W., Auerswald, K., and Bunzl, K.: Estimation of soil erosion and deposition rates at an agricultural site in Bavaria, Germany, as derived from fallout radiocesium and plutonium as tracers, *Naturwissenschaften*, 89, 43-46, 2002.



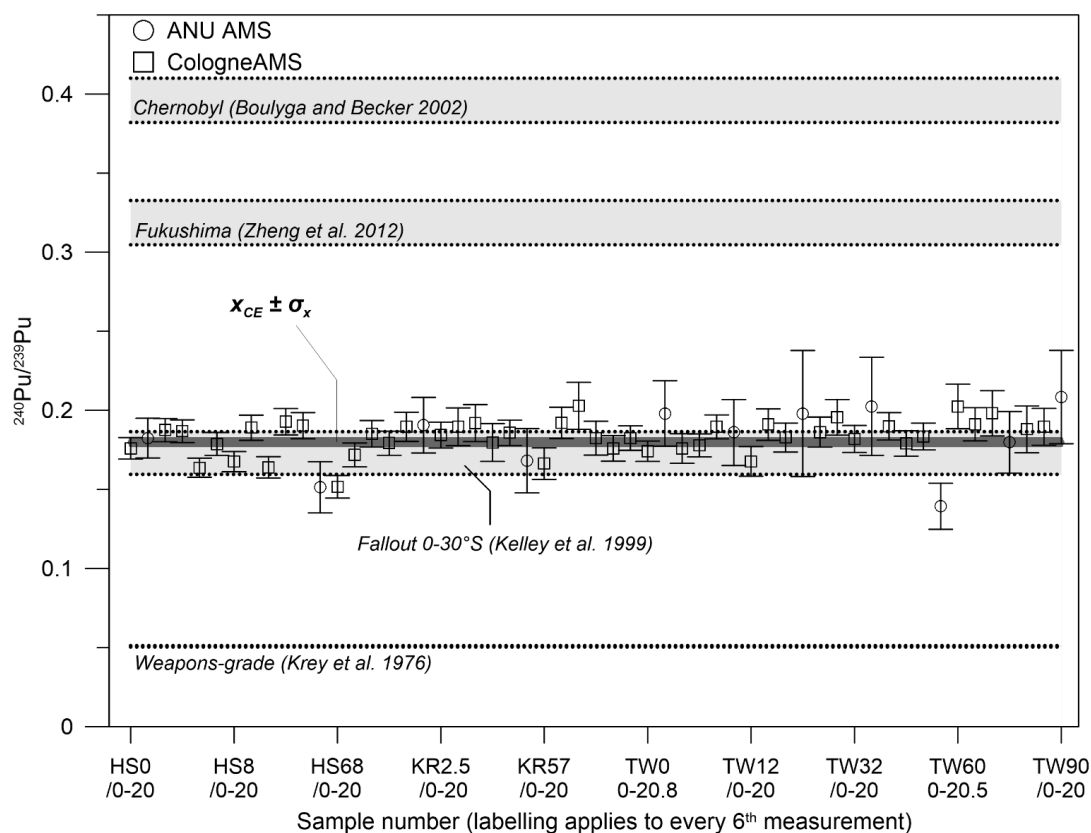
- 630 Smith, B. S., Child, D. P., Fierro, D., Harrison, J. J., Heijnis, H., Hotchkis, M. A. C., Johansen, M. P., Marx, S., Payne, T. E., and Zawadzki, A.: Measurement of fallout radionuclides, $^{239,240}\text{Pu}$ and ^{137}Cs , in soil and creek sediment: Sydney Basin, Australia, *Journal of Environmental Radioactivity*, 151, 579-586, 2016a.
- Smith, P., House, J. I., Bustamante, M., Sobocká, J., Harper, R., Pan, G., West, P. C., Clark, J. M., Adhya, T., Rumpel, C., Paustian, K., Kuikman, P., Cotrufo, M. F., Elliott, J. A., McDowell, R., Griffiths, R. I., Asakawa, S., Bondeau, A., Jain, A. K., Meersmans, J., and Pugh, T. A. M.: Global change pressures on soils from land use and management, *Global Change Biology*, 22, 1008-1028, 2016b.
- 635 Soil Survey Staff: Keys to Soil Taxonomy, USDA-Natural Resources Conservation Service, Washington, DC., 2014.
- Sokol, N. W., Sanderman, J., and Bradford, M. A.: Pathways of mineral-associated soil organic matter formation: Integrating the role of plant carbon source, chemistry, and point of entry, *Glob Chang Biol*, 25, 12-24, 2019.
- 640 Solomon, D., Lehmann, J., Lobe, I., Martinez, C. E., Tveitnes, S., Du Preez, C. C., and Amelung, W.: Sulphur speciation and biogeochemical cycling in long-term arable cropping of subtropical soils: evidence from wet-chemical reduction and S K-edge XANES spectroscopy, *European Journal of Soil Science*, 56, 621-634, 2005.
- UN Scientific Committee on the Effects of Atomic Radiation: Sources and effects of ionizing radiation. United Nations Scientific Committee on the Effects of Atomic Radiation. Volume 1: Sources, UN, New York, 89 pp., 2000.
- United Kingdom Atomic Energy Authority (UKAEA): Certified Nuclear Reference Material No.: UK Pu 5/92138. H.L. Chemistry Division, Oxfordshire OX11 0RA.
- 645 Van Pelt, R. S., Zobeck, T. M., Ritchie, J. C., and Gill, T. E.: Validating the use of ^{137}Cs measurements to estimate rates of soil redistribution by wind, *Catena*, 70, 455-464, 2007.
- von Sperber, C., Stallforth, R., Du Preez, C., and Amelung, W.: Changes in soil phosphorus pools during prolonged arable cropping in semiarid grasslands, *European Journal of Soil Science*, 68, 462-471, 2017.
- 650 Vos, H. C., Fister, W., Eckardt, F. D., Palmer, A. R., and Kuhn, N. J.: Physical Crust Formation on Sandy Soils and Their Potential to Reduce Dust Emissions from Croplands, *Land*, 9, 503, 2020.
- Wallbrink, P. J., Walling, D. E., and He, Q.: Radionuclide Measurement Using HPGe Gamma Spectrometry. In: *Handbook for the Assessment of Soil Erosion and Sedimentation Using Environmental Radionuclides*, Zapata, F. (Ed.), Springer Netherlands, Dordrecht, 2003.
- 655 Wilding, L.: Spatial variability: its documentation, accomodation and implication to soil surveys, 1985, 166-194.
- Xu, Y., Qiao, J., Hou, X., and Pan, S.: Plutonium in Soils from Northeast China and Its Potential Application for Evaluation of Soil Erosion, *Scientific Reports*, 3, 3506, 2013.
- Xu, Y., Pan, S., Wu, M., Zhang, K., and Hao, Y.: Association of Plutonium isotopes with natural soil particles of different size and comparison with ^{137}Cs , *Science of The Total Environment*, 581-582, 541-549, 2017.
- 660 Yan, H., Wang, S., Wang, C., Zhang, G., and Patel, N.: Losses of soil organic carbon under wind erosion in China, *Global Change Biology*, 11, 828-840, 2005.
- Zapata, F.: *Handbook for the assessment of soil erosion and sedimentation using environmental radionuclides*, Springer, 2002.
- Zheng, J., Tagami, K., Watanabe, Y., Uchida, S., Aono, T., Ishii, N., Yoshida, S., Kubota, Y., Fuma, S., and Ihara, S.: Isotopic evidence of plutonium release into the environment from the Fukushima DNPP accident, *Scientific Reports*, 2, 304, 2012.
- 665



670 **Figure 1: Topographic map of the Republic of South Africa and the state territory of the Kingdom of Lesotho. Sampling locations**
675 **are highlighted by tear pins. Administratively, the investigated sites are located within the Free State Province of the Republic of**
South Africa. The province largely stretches the Highveld ecoregion, which resembles an elevated, open grassland plain landscape.



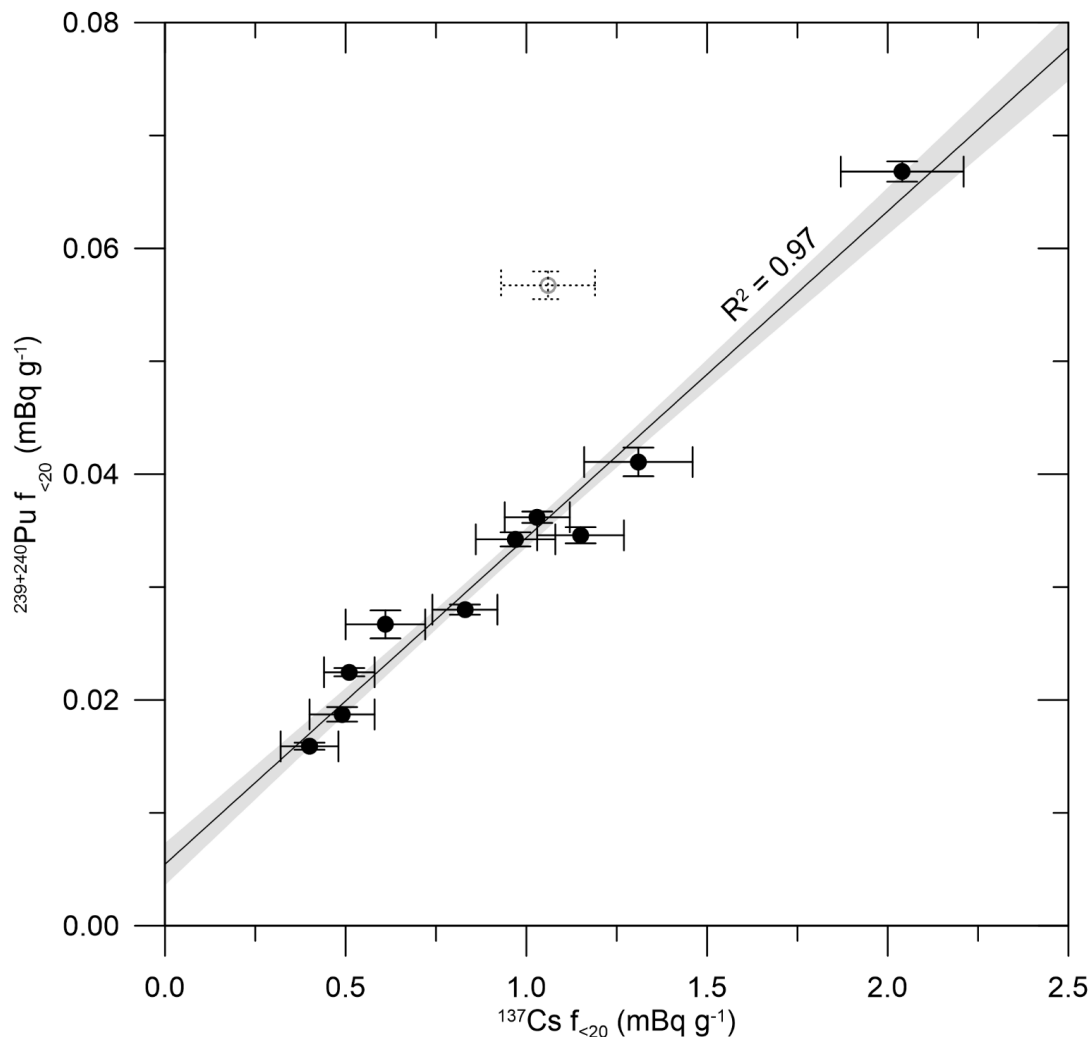
680 Figure 2: Changes in topsoil fallout concentrations (A) and soil organic carbon (SOC) content (B; Lobe et al., 2001) in the soil
 fraction <math><20\ \mu\text{m}</math> over time, and correlation of the two variables (C). The concentrations in cultivated soils are shown relative to those
 found in adjacent native grassland soils (i.e., 100% at $t = 0$). The mono-exponential regression (thin black line, enveloped by grey
 685 68% confidence interval) in panel (A) indicates the approach towards a concentration equilibrium level after about 25-45 years of
 cropping. By that time, about 50-60% of the initial $^{239+240}\text{Pu}$ concentration has been lost. The extrapolated post-32 years cropping
 equilibrium level is indicated by the dashed line. The relationship between $^{239+240}\text{Pu}$ and SOC in the clay and silt fractions indicate
 that the decrease of SOC can be traced by measuring $^{239+240}\text{Pu}$ in soil fines (C). Most plutonium samples depict replicate
 measurements; the corresponding concentrations are weighted means and the uncertainties either dominated by AMS counting
 statistics (weighted mean error) or external sources of uncertainty (standard error). For single measurements, the 1σ measurement
 uncertainty provided by the AMS facilities dominates the final uncertainty. All greyed out data points with dashed error bars denote
 690 those samples that were taken from plots with more than 32 years of cultivation history (for discussion see text). Filled circles denote
 samples from the Harrismith (HS) agroecosystem; filled triangle those from the Kroonstad (KR) agroecosystem and filled diamonds
 those from the Tweespruit (TW) agroecosystem.



695 **Figure 3:** $^{240}\text{Pu}/^{239}\text{Pu}$ of all samples measured (including replicates; error bars denote 1σ AMS measurement uncertainties). The
 weighed mean x_{CE} of all ratios is 0.180 ± 0.002 (thick black line includes the standard error σ_x). The weighed mean thus plots within
 the range of ^{239}Pu and ^{240}Pu sourced from global fallout for the latitudinal band $0-30^\circ\text{S}$ (0.173 ± 0.014 , 1σ) as constrained by Kelley
 et al. (1999). Other FRN sources are characterised by different $^{240}\text{Pu}/^{239}\text{Pu}$, e.g. when originating from the Chernobyl nuclear power
 700 plant (NPP) accident (here shown as the 1σ range of the mean; 0.396 ± 0.014) cited from Boulyga and Becker (2002), Fukushima
 NPP accident (1σ of the mean, i.e. 0.319 ± 0.014 of three surface soil samples taken 25–32 km away from the power plant) calculated
 from Zheng et al. (2012), or when originating from weapons-grade plutonium (Nevada National Security Site, GMX area, 1σ of the
 mean – 0.051 ± 0.000) cited from Krey et al. (1976).

705

710



715 **Figure 4: Correlation of ^{137}Cs and $^{239+240}\text{Pu}$ topsoil activities.** ^{137}Cs data are shown with 1σ uncertainties (which equal the estimated measurement errors). $^{239+240}\text{Pu}$ activities were mostly measured in replicate, and the corresponding concentrations are weighted means and the uncertainties either dominated by AMS counting statistics (weighted mean error) or external sources of uncertainty (standard error). For single measurements, the 1σ measurement uncertainty provided by the AMS facilities dominates the final uncertainty. The majority of samples overlap with the linear regression (black line) and its 68% confidence interval (in grey). Sample HS0/0-20 has been excluded from the regression (greyed out; for discussion see text). The extrapolated regression intersects the
720 y -axis at about $0.0050 \text{ mBq g}^{-1}$ (0.50 mBq kg^{-1} ; unit conversion to mBq g^{-1} due to lower level precision achieved by γ spectrometry). ^{137}Cs data have been decay-corrected to February 2012 (the time of measurement).

725



730

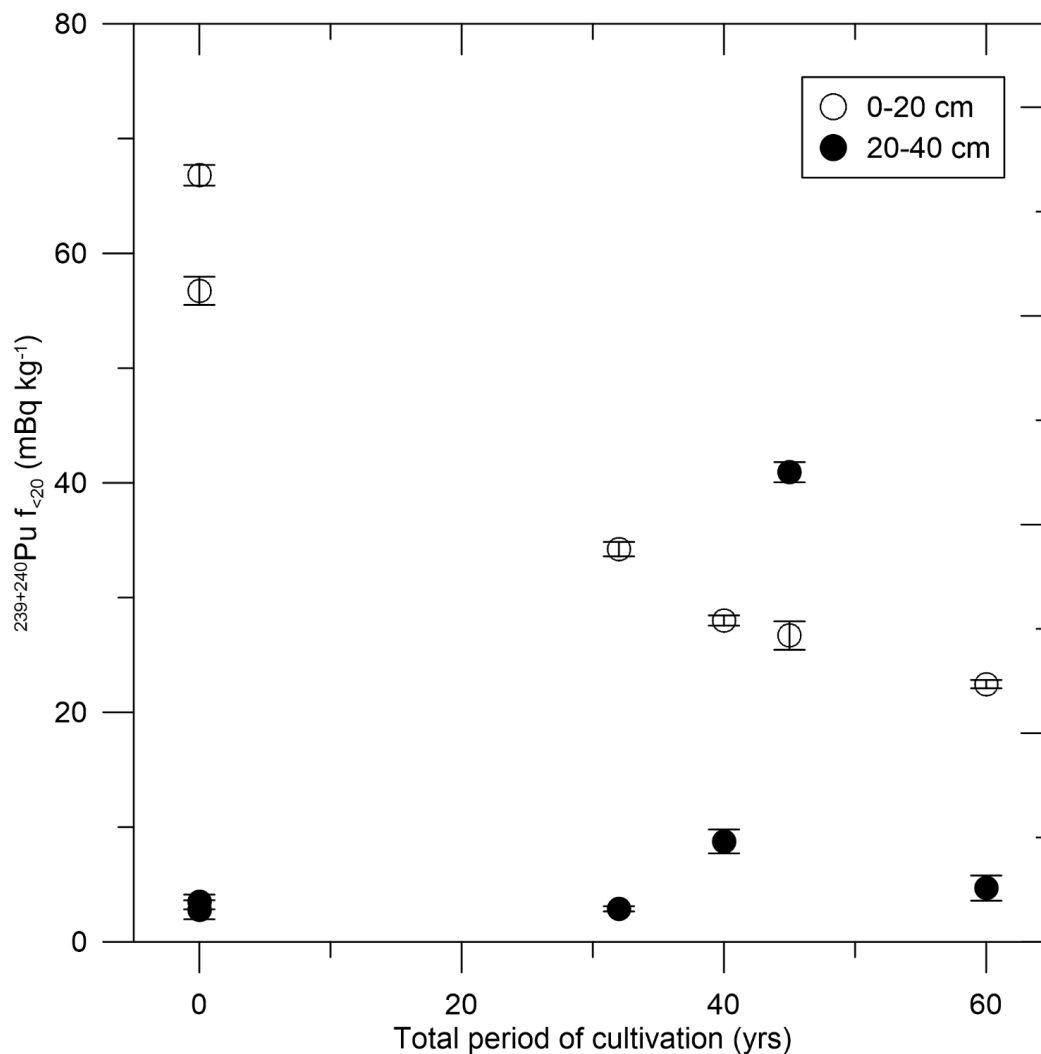


Figure 5: $^{239+240}\text{Pu}$ concentrations at depth (20–40 cm) as compared to corresponding topsoil activities (0–20 cm). The analysis of plutonium activities at depth has been conducted for $n = 6$ samples, belonging to the agroecosystems Tweespruit (0, 32, 40, and 60 years of cultivation) and Harrismith (0 and 45 years of cultivation). At all sites but HS45, the nuclide concentration is significantly lower at depth than close to the surface. Error bars are 1σ uncertainties (see Fig. 2 for details).

735

740

745



Table 1: Agroecosystem details.

	Harrismith	Kroonstad	Tweespruit
Abbreviation	HS	KR	TW
Number of plots investigated	9	7	8
Mean centre	28.04°E, 28.38°S	27.01°E, 27.90°S	27.08°E, 29.24°S
Mean elevation	1728 m a.s.l.	1451 m a.s.l.	1616 m a.s.l.
Mean distance between plots	52.5 km	14.4 km	13.7 km
Climate region	Cwb	Cwa, Cwb	Cwb
Soil texture	Sandy loam	Loamy sand	Sandy loam
Ploughing depth	mostly 20 cm ^b	20 cm	20 cm
Soil type	Plinthic Lixisols/Typic Plinthustalfs		
Crops	Maize, wheat, sunflower		
(Average grain yields)	(2.2-3.8, 1.2-2.8, 2.2-3.8 t ha ⁻¹)		

750 The sampling sites were assigned to climate regions according to Beck et al. (2018). Cwa – Temperate, dry winter, hot summer; Cwb – temperate, dry winter, warm summer (in KR agroecosystem sample site KR57 only). The ploughing depth was reported to be 40 cm in HS30 and HS68. Soil types according to World Soil Reference Base (IUSS Working Group WRB, 2015) and Soil Survey Staff (2014). Average grain yields valid for the time of sampling (1998), cited from Lobe et al. (2001).

755

760

765

770

775



Table 2: FRN concentrations.

Sample ID	n	²³⁹⁺²⁴⁰ Pu			¹³⁷ Cs	
		(mBq kg ⁻¹)	(%)		(Bq kg ⁻¹)	
HS 0 /0-20	2	56.73 ± 1.23	100.0	± 2.2	1.06 ± 0.13	
HS 3.5 /0-20	1	51.66 ± 1.02	91.1	± 2.7	-	
HS 5 /0-20	2	49.44 ± 1.36	87.2	± 3.1	-	
HS 8 /0-20	2	42.98 ± 0.87	75.8	± 2.2	-	
HS 10 /0-20	2	28.68 ± 1.23	50.6	± 2.4	-	
HS 30 /0-20	2	25.95 ± 0.39	45.7	± 1.2	-	
HS 45 /0-20	1	26.69 ± 1.24	47.1	± 2.4	0.61 ± 0.11	
HS 68 /0-20	2	23.90 ± 1.88	42.1	± 3.4	-	
HS 90 /0-20	2	27.85 ± 0.58	49.1	± 1.5	-	
KR 0 /0-20	2	34.59 ± 0.72	100.0	± 2.1	1.15 ± 0.12	
KR 2.5 /0-20	1	34.57 ± 0.75	99.9	± 3.0	-	
KR 20 /0-20	2	23.27 ± 0.48	67.3	± 2.0	-	
KR 30 /0-20	1	26.58 ± 0.81	76.8	± 2.8	-	
KR 40 /0-20	2	15.90 ± 0.31	46.0	± 1.3	0.40 ± 0.08	
KR 57 /0-20	2	22.07 ± 1.44	63.8	± 4.4	-	
KR 98 /0-20	2	14.49 ± 0.31	41.9	± 1.3	-	
TW 0 /0-20	3	66.80 ± 0.90	100.0	± 1.3	2.04 ± 0.17	
TW 8.5 /0-20	4	41.09 ± 1.27	61.5	± 2.1	1.31 ± 0.15	
TW 12 /0-20	4	36.19 ± 0.51	54.2	± 1.1	1.03 ± 0.09	
TW 22 /0-20	1	33.47 ± 0.82	50.1	± 1.4	-	
TW 32 /0-20	3	34.23 ± 0.63	51.2	± 1.2	0.97 ± 0.11	
TW 40 /0-20	4	28.00 ± 0.45	41.9	± 0.9	0.83 ± 0.09	
TW 60 /0-20	4	22.46 ± 0.37	33.6	± 0.7	0.51 ± 0.07	
TW 90 /0-20	3	18.73 ± 0.65	28.0	± 1.0	0.49 ± 0.09	
HS 0 /20-40	2	2.80 ± 0.83	4.9	± 1.5	-	
HS 45 /20-40	2	40.93 ± 0.88	153.3	± 7.8	-	
TW 0 /20-40	3	3.48 ± 0.64	5.2	± 1.0	-	
TW 32 /20-40	1	2.88 ± 0.23	8.4	± 0.7	-	
TW 40 /20-40	1	8.76 ± 1.04	31.3	± 3.8	-	
TW 60 /20-40	1	4.69 ± 1.11	20.9	± 4.9	<i>below detection limit</i>	

780 Sample labelling includes the abbreviation of the sample agroecosystem, years of cultivation and sampling depth interval: HS -
Harrismith, KR - Kroonstad, TW - Tweespruit. The number *n* of ^{239,240}Pu replicate measurements includes both CologneAMS and
ANU AMS measurement replicates. The quoted plutonium concentrations from replicate measurements are weighted means and
the uncertainties either dominated by AMS counting statistics (weighted mean error) or external sources of uncertainty (standard
error). For single measurements, the 1σ measurement uncertainty provided by the AMS facilities dominates the final uncertainty.
785 Percentual concentrations of the topsoil samples are normalised to the undisturbed reference sample for each agroecosystem. For
the depth samples, the percentage values denote the difference against the corresponding topsoil samples. ¹³⁷Cs data uncertainties
equal 1σ measurement errors arising from μ spectrometry conducted at CSIRO. All ¹³⁷Cs has been corrected for decay to February
2012.

790